ELSEVIER

Journal of Nuclear Materials 247 (1997) 76–81

journal of nuclear materials

# Recovery behavior of thermal conductivity in irradiated $UO_2$ pellets

Masaki Amaya *, Mutsumi Hirai

*Nippon Nuclear Fuel Development Co., Ltd., 2163 Narita-cho, Oarai-machi, Higashi-ibaraki-gun, Ibaraki-ken, 311-13, Japan*

**Abstract**

The thermal conductivity of irradiated $UO_2$ pellets was analyzed based on the results of X-ray diffraction and TEM observations. The thermal conductivity degradation of irradiated $UO_2$ pellets may be classified as due to the effects of soluble FPs, irradiation-induced point defects and extended defects such as microbubbles. A thermal conductivity formula was obtained by using Klemens' theory. The formula could express the thermal conductivity of $UO_2$ pellets containing impurities, irradiation-induced point defects, and irradiation-induced microbubbles. The thermal conductivity recovery of the irradiated $UO_2$ pellets which was observed in out-of-pile data at about 1100 K could be expressed by considering the phonon scattering of irradiation-induced point defects and the lattice parameter recovery of irradiated $UO_2$. © 1997 Elsevier Science B.V.

## 1. Introduction

Thermal conductivity of fuel pellets is one of the most important thermal properties necessary to calculate fuel temperature. For high burnup fuels, fission products (FPs) accumulate in fuel pellets. The increased crystal lattice strain caused by irradiation-induced point defects and formation of microbubbles are also observed in irradiated $UO_2$ pellets [1–3]. The pellet thermal conductivity is affected by these impurities and irradiation-induced defects, and it is necessary to evaluate the quantitative changes in the thermal conductivity due to impurities and irradiation defects.

The thermal conductivity of $UO_2$ pellets irradiated in a material test reactor up to $10^{21}$ fissions $cm^{-3}$ has been measured [4–12] and it was found that the thermal conductivity was degraded at temperatures below about 800 K with increasing burnup, and that thermal conductivity recovery occurred. However, for (U, Pu)$O_2$ irradiated up to burnup 35 GWd/tU in an FBR [13,14], the burnup dependence of the thermal conductivities and the thermal conductivity recovery were not clear.

The thermal conductivity degradation by soluble FPs has already been formulated [15,16], but the effects of crystal lattice strain caused by irradiation-induced point defects and that of microbubbles were not quantified. In this paper, the thermal conductivity of irradiated $UO_2$ pellets were evaluated based on the literature data. The evaluation were used to quantify the effects of irradiation-induced defects on the thermal conductivity and to explain the thermal conductivity recovery behavior.

## 2. Thermal conductivity of irradiated $UO_2$

Thermal conductivity of irradiated $UO_2$ pellets is affected by irradiation conditions such as irradiation temperature and irradiation dose[4], because the structure of the irradiation-induced defects changes with these irradiation conditions [4]. Measured temperature ranges used by different researchers are summarized in Table 1.

Ross [5] measured the thermal conductivities of irradiated samples by using a longitudinal heat flow method. A thermal conductivity degradation of 26% at 333 K was obtained for the samples of $2 \times 10^{16}$ fissions $cm^{-3}$ relative to unirradiated $UO_2$.

Daniel et al. [6] measured the thermal conductivities of $UO_2$ by using a heat flow method. They observed degradation of about 50% at room temperature and thermal conductivity recovery at 423 K, 573 K and 1073 K at $1.1 \times 10^{19}$ fissions $cm^{-3}$. Above $1.4 \times 10^{19}$ fissions $cm^{-3}$, the

* Corresponding author. Tel.: +81-29 266 2131; fax: +81-29 266 2589; e-mail: amaya@nfd.co.jp.


*PII* S0022-3115(97)00065-2

Table 1
Summary of irradiation doses and irradiation temperatures used by different researchers

| Researchers | Irradiation dose/fission $cm^{-3}$ | Irradiation temperature (K) |
|---|---|---|
| Ross [5] | $2 \times 10^{16}$–$7 \times 10^{18}$ | < 723 |
| Daniel et al. [6] | $1.4 \times 10^{18}$–$1.1 \times 10^{19}$ | < 373 |
| Hawkings and Robertson [7] | $10^{15}$–$10^{18}$ | < 773 |
| Clough and Sayers [8] | $5 \times 10^{17}$–$1.5 \times 10^{19}$ | < 773 |
| Stora et al. [9] | $< 7 \times 10^{17}$ | |
| Daniel and Cohen [10] | $< 28 \times 10^{20}$ | |
| Nakamura et al. [12] | $16 \times 10^{20}$ (63 GWd/tU) | |

thermal conductivities were degraded monotonously in proportion to irradiation dose.

Hawkings and Robertson [7] measured the effective thermal conductivities of fuel elements and observed thermal conductivity degradation of pellets irradiated below 773 K. The degradation tendency above $10^{18}$ fissions $cm^{-3}$ was smaller than that below $10^{16}$ fissions $cm^{-3}$. They also measured the effective thermal conductivities of stoichiometric $UO_2$ up to 1473 K. Their results showed a clear thermal conductivity degradation due to irradiation-induced defects below 1000 K and a tendency for the thermal conductivity to saturate at around 3.5 W $m^{-1}$ $K^{-1}$ below 1000 K.

Clough and Sayers [8] measured the thermal conductivities of the fuel pellets directly by using a radial heat flow method. They observed thermal conductivity degradations of 50% and 20% at irradiation temperatures of 453 K and 593 K, respectively, and no apparent thermal conductivity changes at an irradiation temperature of 793 K, at $1.5 \times 10^{19}$ fissions $cm^{-3}$. They annealed samples with irradiation doses from $10^{18}$ to $5 \times 10^{18}$ fission $cm^{-3}$ and found thermal conductivity degradations due to irradiation-induced defects formed at 453 K and 593 K were recovered at 723 K and 1023 K, respectively. However, no thermal conductivity recovery was observed for samples above $10^{19}$ fissions $cm^{-3}$. They also observed no apparent thermal conductivity degradation in the temperature region from 773 to 1873 K below $4 \times 10^{19}$ fissions $cm^{-3}$.

Stora et al. [9] measured the effective thermal conductivities of fuel pellets and observed no apparent thermal conductivity degradation in the temperature region from 773 to 1573 K below $7 \times 10^{17}$ fissions $cm^{-3}$.

Daniel and Cohen [10] measured the effective thermal conductivity of $UO_2$ pellets and observed thermal conductivity degradations of 20% and 50% for burnups of $5 \times 10^{20}$ and $28 \times 10^{20}$ fissions $cm^{-3}$, respectively, in comparison with unirradiated $UO_2$.

Marchandise [11] analysed the thermal conductivity data of Daniel and Cohen [10] and reported the thermal conductivities of 40 GWd/tU burnup pellets were degraded to those of 73% and 90% for unirradiated ones at 773 and 1773 K, respectively.

Nakamura et al. [12] measured the thermal diffusivities of irradiated $UO_2$ pellets, which were prepared from a fuel rod irradiated in a material test reactor up to 63 GWd/tU, by using a laser flash method, and observed thermal diffusivity recovery due to sample annealing in the temperature region above about 1000 K.

Fig. 1 compares the thermal conductivities for irradiated $UO_2$ as reported in these major studies.

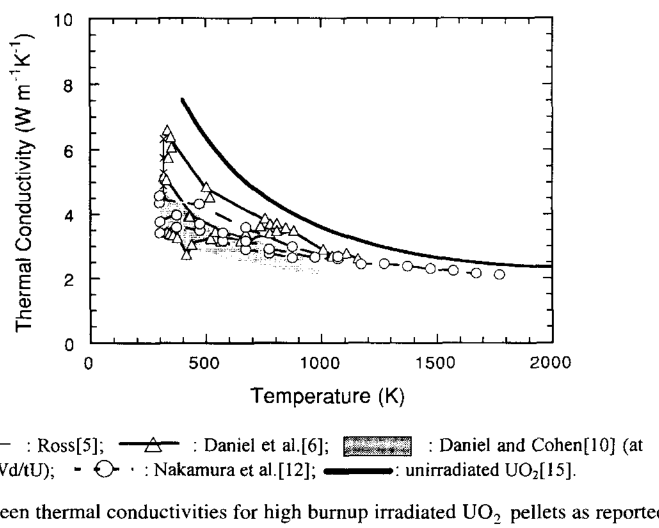


Fig. 1. Comparison between thermal conductivities for high burnup irradiated $UO_2$ pellets as reported in major studies.

## 3. Data for estimation of thermal conductivities for irradiated $UO_2$ pellets

We used the following two reports of thermal conductivity data for estimating the thermal conductivities of high burnup irradiated $UO_2$ pellets above $5 \times 10^{20}$ fission cm$^{-3}$ (20 GWd/tU): (1) Daniel and Cohen [10] and (2) Nakamura et al. [12].

Daniel and Cohen [10] obtained the following equation to express the effective thermal conductivities of $UO_2$ pellets irradiated up to $28 \times 10^{20}$ fissions cm$^{-3}$

$$\lambda_{irr} = 1/\left(\lambda_0^{-1} + X + fZ\right), \tag{1}$$

where $\lambda_{irr}$ is the in-pile thermal conductivity of $UO_2$ pellet; $\lambda_0$ is the thermal conductivity of unirradiated $UO_2$ pellet; $X$ is the thermal resistivity due to irradiation defects which occurred before the first in-pile measurements were made; $f$ is the fission depletion in $10^{20}$ fissions cm$^{-3}$; and $Z$ is the thermal resistivity increase per $10^{-20}$ fissions$^{-1}$ cm$^3$. The initial average fuel density was 10.6 g/cm$^3$ (97% theoretical density) and the initial average fuel porosity was 3%. We assumed that the fuel average porosity was unchanged during irradiation.

Nakamura et al. [12] reported only the thermal diffusivities of irradiated $UO_2$ (burnup: 63 GWd/tU) samples. Therefore, we converted the thermal diffusivity into the thermal conductivity using the following equation:

$$\lambda = \alpha C_p \rho, \tag{2}$$

where $\lambda$ is the thermal conductivity of the sample; $\alpha$ is the thermal diffusivity of the sample; $C_p$ is the specific heat capacity; and $\rho$ is the sample density. They did not state the sample density explicitly. Therefore, we assumed that the initial sample density was 10.4 g/cm$^3$ (95% theoretical density), the initial sample porosity was 5%, and the sample porosity was unchanged during irradiation. Since the difference between the specific heat capacity of $UO_2$ and soluble simulated FP-doped $UO_2$ is about 2% even at simulated burnup 90 GWd/tU [15], we used the specific heat capacity of $UO_2$ [17] as that of the irradiated $UO_2$ sample.

## 4. Discussion

After ceramic materials such as $Al_2O_3$, SiC and AlN are irradiated, their thermal conductivities are decreased and are close to being independent of the temperature [18,19]. From the discussions using Price's theory [20], the decrease of thermal conductivities was caused by the irradiation-induced impurities, point defects, dislocations and vacancy/interstitial clusters. This fact indicates that it is necessary to consider the effects of irradiation-induced defects on thermal conductivities as well as those of impurities, in order to analyse the thermal conductivity changes of irradiated $UO_2$ pellets.

### *4.1. Recovery behavior of irradiation-induced defects in irradiated $UO_2$*

The temperature ranges for irradiation defect recovery and microbubble growth, based on Refs. [1–3], are summarized in Fig. 2. We considered that the thermal conductivity changes of irradiated $UO_2$ pellets could be classified as to the effects of irradiation-induced point defects, fission products and irradiation-induced microbubbles.

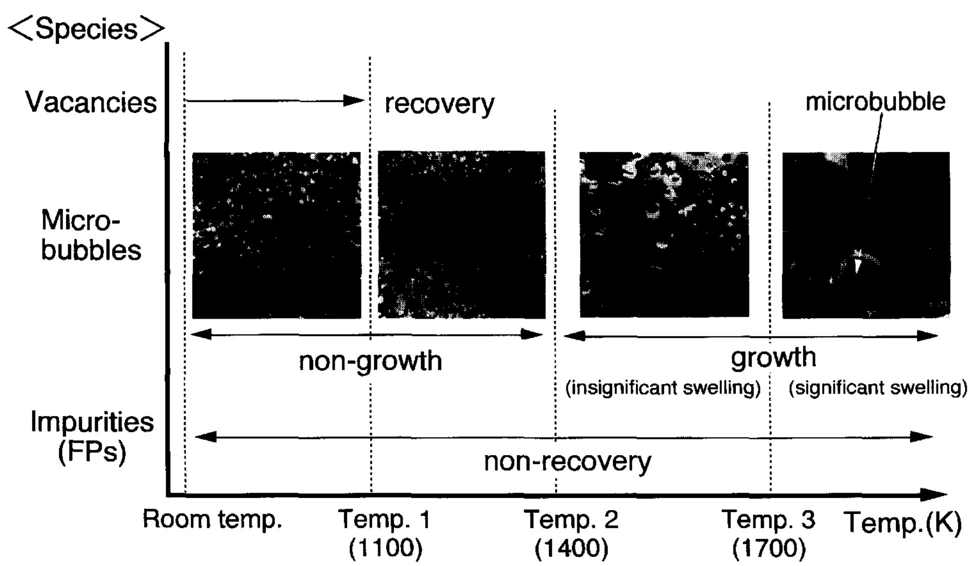


Fig. 2. The temperature range for irradiation defect recovery and microbubble growth based on Refs. [1,1,3].

### 4.2. The effects of point defects and extended defects on thermal conductivity of $UO_2$ pellet

The thermal conductivity of $UO_2$ pellet containing point defects, such as impurities (FPs, $Gd^{3+}$, $U^{5+}$), is expressed as follows [15,21–25]:

$$\lambda_p = \lambda_0 \tan^{-1} x / x + CT^3, \tag{3}$$

where $\lambda_p$ is the thermal conductivity of $UO_2$ pellet containing point defects; $\lambda_0$ is the thermal conductivity of pure $UO_2$; $x$ is the phonon scattering parameter which expresses the degree of phonon scattering by point defects; $C$ is a coefficient which express the other effects except thermal conductivity by phonons; and $T$ is the temperature in K. From our previous work [15], the phonon scattering parameter of $UO_2$ pellets, $x$, can be expressed using the concentration of impurities as follows:

$$x = \sum_i [D_i y_i]^{1/2} \lambda_0^{1/2}, \tag{4}$$

where $D_i$ is the coefficient which expresses the effect of impurity $i$ on the thermal conductivity; and $y_i$ is the metallic fraction of $i$.

The thermal conductivity degradation of $UO_2$ pellet by extended defects is expressed as follows [23]:

$$\lambda_x / \lambda_0 = 1 - \chi_0 \tan^{-1}(1/\chi_0), \tag{5}$$

where $\lambda_x$ is the thermal conductivity of $UO_2$ pellet which has extended defects; $\chi_0$ is the parameter which expresses the degree of phonon scattering by the extended defects, and $\chi_0$ can be expressed as follows:

$$\chi_0 = [3\alpha_0/(uL)]^{1/2}, \tag{6}$$

where $\alpha_0$ is the thermal diffusivity of pure $UO_2$ [26], $\alpha_0 = 1/(0.46586 + 0.087386T)$ in $cm^2/s$; $u$ is the group velocity of phonons in $UO_2$ crystal, $u = 3.09 \times 10^5$ cm/s, which was evaluated from the elastic constants [17]. $L$ is the mean free path of a phonon in $UO_2$ and it is expressed as follows:

$$1/L = NA = N\pi R^2, \tag{7}$$

where $N$ is the number density of extended defects; $A$ is the cross-section of an extended defect; and $R$ is the radius of an extended defect.

High concentrations of point defects and extended defects coexist in high burnup fuel pellets. According to Klemens' theory [21–23], the phonon thermal conductivity of ceramics is expressed as follows using phonon mean free path

$$\lambda = \frac{1}{3} \int_0^{\omega_D} \{C(f) v(f) l(f)\} \mathrm{d}f, \tag{8}$$

where $C(f)$ is the heat capacity of a material per unit volume; $v(f)$ is the velocity of a lattice wave and $l(f)$ is the phonon mean free path. $l$ is changed due to the phonon scattering mechanism and each contribution to the thermal conductivity in high burnup fuel pellets is expressed as follows:

$$1/l = 1/l_i + 1/l_p + 1/l_x, \tag{9}$$

where $l_i$ is the intrinsic phonon scattering mean free path due to the Umklapp process; $l_p$ is the phonon scattering mean free path due to point defects; and $l_x$ is the phonon scattering mean free path due to extended defects.

Substituting Eq. (9) into Eq. (8), we obtained the following equation after considering the lattice vibration frequency dependence of each phonon scattering process [22]:

$$\lambda_s = \lambda_0 K \left[ \theta_1 \tan^{-1}(1/\theta_1) - \theta_2 \tan^{-1}(1/\theta_2) \right] + CT^3, \tag{10}$$

where

$$K = 1/\sqrt{1 - 4\chi_0^2 x^2}, \tag{11}$$

$$\theta_1 = \left( \sqrt{\tfrac{1}{2} + x\chi_0} + \sqrt{\tfrac{1}{2} - x\chi_0} \right) / \sqrt{2}\, x, \tag{12}$$

$$\theta_2 = \left( \sqrt{\tfrac{1}{2} + x\chi_0} - \sqrt{\tfrac{1}{2} - x\chi_0} \right) / \sqrt{2}\, x. \tag{13}$$

In this paper, we assumed that the point defects were soluble FP atoms and the irradiation-induced point defects, and the extended defects were microbubbles.

The lattice strains formed by the irradiation-induced point defects recovered at around 900 K [1] and the concentration of the soluble FP is increased nearly in proportion to burnup. According to the X-ray diffraction results of Une et al. [27], the lattice parameters of irradiated $UO_2$ pellets also increased nearly in proportion to burnup below about 50 GWd/tU due to the accumulation of irradiation-induced point defects. Therefore, we made the following assumptions:

(1) the concentration and the lattice strain of the irradiation- induced point defects are increased in proportion to burnup,

(2) the recovering process of the irradiation induced point defects can be expressed using the Weibul function and

(3) the degradation effect of thermal conductivity due to irradiation-induced point defects is equivalent to that of FP atoms.

Using these assumptions, Eq. (4) can be rewritten as

$$x = \left[ D_{FP} \cdot E\{1 + A \exp(-(t/t_r)^n)\} \right]^{1/2} \lambda_0^{1/2}, \tag{14}$$

where $E$ is the burnup in GWd/tU; $t$ is the temperature in °C; $t_r$ is the temperature of the recovering stage in °C; $n$ is a coefficient. $D_{FP}$ is expressed by the following equation based on our previous work [15]:

$$D_{FP} = 6.69 \times 10^{-3} \exp(-3.28 \times 10^{-4} T). \tag{15}$$

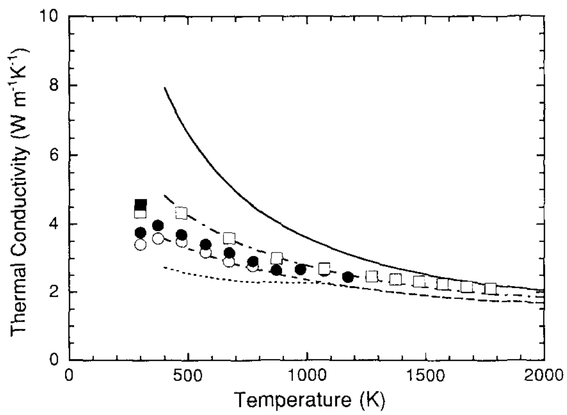


---, — —, —-—, —: calculated values from eq.(11).
---: A=1, R =1nm; — — : A=0, R =1nm; — - — : soluble FP doped $UO_2$ (corresponding to 63GWd/tU[15]); —: unirradiated $UO_2$.
○, ●, □, ■: measured values by Nakamura et al.[12].
○: 1st run; ●: 2nd run; □: 3rd run; ■: 4th run.

Fig. 3. Comparison between the thermal conductivities of irradiated $UO_2$ pellets calculated from Eq. (10) and the measured ones by Nakamura et al. [12].

The coefficient $A$ shows the phonon-scattering effects of irradiation-induced point defects and we assumed that $A = 1$ for the 1st- run data of Nakamura et al. [12] and $A = 0$ for all data of Nakamura et al. after being annealed above 1100 K. In order to express the lattice parameter changes obtained by Nogita et al. [1], we used 650 as $t_r$ and 5 as $n$.

The relationship between the number density and the radius of microbubbles was obtained by Kashibe et al. [14] for irradiated $UO_2$ pellets which had burnup above about 6 GWd/tU, and is expressed as follows:

$$N = 10^{19.1}(2R)^{-2.6}, \qquad (16)$$

where $N$ is the number density of microbubbles in $cm^{-3}$; and $R$ is the radius of microbubbles in nm.

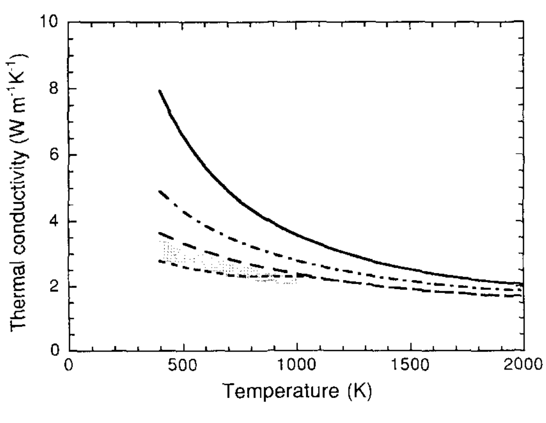


---, — —, —-—, —: calculated values from eq.(11).
---: A=1, R =1nm; — — : A=0, R =1nm; — - — : soluble FP doped $UO_2$ (corresponding to 60GWd/tU[15]); —: unirradiated $UO_2$.
▒ : calculated values from eq.(1) by Daniel and Cohen[10].

Fig. 4. Comparison between the thermal conductivities of irradiated $UO_2$ pellets (burnup: 60 GWd/tU) calculated from Eq. (10) and the calculated ones from Eq. (1) by Daniel and Cohen [10].

In TEM observations [1], the radii of micro-bubbles were from 1 nm to 10 nm for as-irradiated samples and about 10 nm for samples after annealing at 1300 K. To calculate the thermal conductivity of irradiated $UO_2$ pellets, it was necessary to evaluate the radius of microbubble, $R$, and we assumed that $R$ was 1 nm for as-irradiated samples and before being annealed at 1300 K.

Fig. 3 compares the values calculated using Eq. (10) with values measured by Nakamura et al. [12]. The calculated values were slightly lower than measured ones. However, the recovery behaviors of the thermal conductivity with temperature were in good agreement with each other. The difference between calculated and measured values may be caused by the sampling position of each sample for each examination, because the annealing conditions of irradiation-induced defects and the microstructure of samples depend on the sampling position. Since Nakamura et al. [12] did not indicate the sampling position clearly, we found it necessary to adjust the coefficients in Eq. (10), considering the irradiation temperature at the sampling position.

The measured values are close to the thermal conductivity of soluble FP-doped $UO_2$ [15] after being annealed at 1200 K. Probably, the effects of irradiation-induced point defects on the thermal conductivity had almost vanished at around 1000 K, in consideration of X-ray diffraction results [1].

On the other hand, Daniel and Cohen [10] did not observe clear thermal conductivity recovery of $UO_2$ fuel pellets for the in-pile condition, and they reported that the coefficient, $Z$, in Eq. (1) was 1.0 and $X$ lay between 0 and 7.4. Fig. 4 compares values calculated using Eq. (10) and Eq. (1) for equivalent burnup of 60 GWd/tU and $X$ between 0 and 7.4. Since they may have averaged the in-pile data of various irradiation conditions, we show their results as the shaded band in Fig. 4. We assumed that the coefficients in Eq. (10) were similar to those Nakamura et al. [12] used. The calculated thermal conductivities based on Eq. (10) are in the shaded band calculated from assuming $X = 0$ and 7.4 in Eq. (1).

## 5. Conclusion

The thermal conductivities of irradiated $UO_2$ pellets were analyzed based on the results of X-ray diffraction and TEM observations.

The thermal conductivity degradations of irradiated $UO_2$ pellets may be classified into the degradation by soluble FPs and irradiation-induced point defects and that by extended defects such as microbubbles. The thermal conductivity formula which could be applied to $UO_2$ pellets containing impurities, irradiation-induced point defects, and irradiation-induced microbubbles was obtained by using Klemens' theory.

The thermal conductivity recovery of the irradiated $UO_2$ pellets which was observed in experimental data [12] at about 1100 K could be expressed by considering the lattice parameter recovery of irradiated $UO_2$.

## Acknowledgements

The authors are indebted to Dr K. Une and Mr K. Nogita for useful discussions.

## References

[1] K. Nogita, K. Une, J. Nucl. Sci. Technol. 30 (1993) 900.
[2] K. Nogita, K. Une, Nucl. Inst. Methods B91 (1994) 301.
[3] S. Kashibe, K. Une, K. Nogita, J. Nucl. Mater. 206 (1993) 22.
[4] Thermal Conductivity of Uranium Dioxide, Technical Report Series No. 59, IAEA, Vienna, 1966.
[5] A.M. Ross, AECL-1096, CRFD-817, 1960.
[6] J.L. Daniel, J. Matolich Jr., H.W. Deem, HW-69945, 1962.
[7] R.C. Hawkings, J.A.L. Robertson, AECL-1733, CRDC-1143, 1963.
[8] D.J. Clough, J.B. Sayers, AERE-R 4690, 1964.
[9] J.P. Stora, B. de B. de Sigoyer, R. Deimas, P. Deschamps, B. Lavand, C. Ringot, CEA-R-2586, 1964.
[10] R.C. Daniel, I. Cohen, WAPD-246, 1964.
[11] H. Marchandise, EUR-4568f, 1970.
[12] J. Nakamura, I. Owada, S. Miyata, T. Furuta, Proc. 1995 Fall Meeting. At. Energy Soc. Jpn., p. 590 (in Japanese).
[13] T. Namekawa, T. Mitsugi, T. Tachibana, S. Yamanouchi, Proc. 35th Conf. Remote Systems Technol., 1987, p. 105.
[14] K. Yamamoto, T. Hirosawa, K. Yoshikawa, K. Morozumi, S. Nomura, J. Nucl. Mater. 204 (1993) 85.
[15] S. Ishimoto, M. Hirai, K. Ito, Y. Korei, J. Nucl. Sci. Technol. 31 (1994) 796.
[16] P.G. Lucuta, Hj. Matzke, R.A. Verrall, H.A. Tasman, J. Nucl. Mater. 188 (1992) 198.
[17] D.L. Hagrman, G.A. Reyman, eds., TREE-NUREG-CR-0497, 1979.
[18] M. Rohde, B. Schultz, J. Nucl. Mater. 173 (1990) 289.
[19] J.C. Corelli, J. Hoole, J. Lazzaro, C.W. Lee, J. Am. Ceram. Soc. 66 (1983) 529.
[20] R.J. Price, J. Nucl. Mater. 46 (1973) 268.
[21] P.G. Klemens, Proc. Phys. Soc. A68 (1955) 1113.
[22] P.G. Klemens, Phys. Rev. 119 (1960) 507.
[23] P.G. Klemens, G.F. Hurley, F.W. Clinard Jr., Proc. 2nd Topical Meeting. Tech. Controlled Nucl. Fusion, Am. Nucl. Soc., ERDA, EPRI 4 vols., Conf. 760935, 1976, p. 957.
[24] M. Hirai, S. Ishimoto, J. Nucl. Sci. Technol. 28 (1991) 995.
[25] M. Amaya, T. Kubo, Y. Korei, J. Nucl. Sci. Technol. 33 (1996) 636.
[26] M. Hirai, J. Nucl. Mater. 173 (1990) 247.
[27] K. Une, K. Nogita, S. Kashibe, M. Imamura, J. Nucl. Mater. 188 (1992) 65.